Indian Journal of Science and Technology, *Vol 8(36), DOI: 10.17485/ijst/2015/v8i36/48589, December 2015*
ISSN (Print) : 0974-6846
ISSN (Online) : 0974-5645

Transient Thermoelastic Analysis of Pressurized Thick Spheres Subjected to Arbitrary Boundary and Initial Conditions

Sanaz Mohammadi, Mohammad Zamani Nejad* and Azam Afshin

Mechanical Engineering Department, Yasouj University, P. O. Box 75914-353, Yasouj, Iran;
m_zamani@yu.ac.ir

Abstract

The current study considers the theoretical transient treatment of pressurized thick-walled hollow spheres while they are subjected to arbitrary boundary and initial conditions. Under generalized assumptions and using the basic thermoelasticity theory, the thermoelastic problem is solved. By utilizing the Eigen function method, generalized Bessel function and separation of variables, an attempt is made to analyze the transient temperature in the one-dimensional state. In this paper, the resultant relations of the present study are capable of being applied to any arbitrary boundary and initial conditions. Temperature, displacement and thermal stresses are plotted in some figures. In this study, the values are arbitrarily chosen.

Keywords: Arbitrary Boundary, Arbitrary Initial Conditions, Thermoelastic, Thick Sphere, Transient

1. Introduction

Shell structures are used in such engineering applications as military, shuttle, marine, automotive, oil, water, and major manufacturing industries. Different types of shells commonly used in the industry are pipes, vessels, fuselages, wings, rockets, car hoods, dome roofs, projectiles, nuclear reactor vessels, silos, bow dams, parachute aircrafts and many more. Stress problems for hollow cylinders and spheres subjected to transient thermoelastic loads are theoretically and practically important. Thus, many research have been carried out in this subject. In solved, the problem of elastic thermal stresses in the transient condition in an elastic solid. In[2] studied transient thermal stress in the spherical shell. In the other study, In[3] investigated the dynamic thermoelastic problem in thick spheres. In[4] studied the thermo-elastic stresses in a non-homogeneous orthotropic solid continuum having a cavity with spherical form. In[5] investigated the dynamic thermo-elastic displacement and stresses distribution in spherical thick shells having fixed boundaries. In[6] scrutinized the thermo-elastic waves in a FG sphere applying the Green-Lindsa theory. In[7] came up with a new approach which could be applied for the purpose of stress analysis of pressurized FGM cylinders, disks or spheres. In[8] studied thermo-elastic analysis in the transient condition for a multilayered thick-walled sphere. In a study by[9], thermo-elastic response in the transient condition of rotating thick-walled cylinder subjected general boundary conditions was obtained. In[10] provided the transient thermoelastic analysis of pressurized rotating disks under arbitrary boundary and initial conditions. Among other things, they obtained transient thermoelastic stresses of homogeneous and isotropic thick spheres under general boundary and initial conditions.

2. Transient Heat Conduction Analysis

In an isotropic hollow sphere with inner and outer radii a and b, respectively in spherical coordinate, the one-dimensional transient heat conduction equation, without heat source, for isotropic bodies is:

** Author for correspondence*

$$\frac{1}{r^2}\frac{\partial}{\partial r}\left(r^2\frac{\partial T}{\partial r}\right)=\frac{\rho C_p}{k}\frac{\partial T}{\partial t} \tag{1}$$

in which the temperature distribution and thermal diffusivity are represented by T(r,t). Moreover, specific heat capacity, mass density and thermal conductivity are represented by c, ρ and k respectively.

The boundary and initial conditions are as:

$$\begin{cases} Boundary\ Condition: \begin{cases} C_{11}T(a,t)+C_{12}\left.\dfrac{\partial T}{\partial r}\right|_{r=a}=g_1 \\ C_{21}T(b,t)+C_{22}\left.\dfrac{\partial T}{\partial r}\right|_{r=b}=g_2 \end{cases} \\ Initial\ Condition: T(r,t)\Big|_{t=0}=T_i(r) \end{cases} \tag{2}$$

Here $T_i(r)$ is the given initial condition and g_m (m = 1,2) and C_{mn} (m,n = 1,2) are constants.

The Equation (3) can be solved applying the separation of variables method, Eigen-function method, and generalized Bessel function

$$T(r,t)=T_h(r,t)+T_s(r) \tag{3}$$

$$\frac{1}{r}\frac{\partial}{\partial r}\left(r\frac{\partial T_s}{\partial r}\right)=0 \tag{4}$$

$$\frac{1}{\kappa}\frac{\partial T_h}{\partial t}=\frac{\partial^2 T_h}{\partial r^2}+\frac{1}{r}\frac{\partial T_h}{\partial r} \tag{5}$$

The boundary conditions for Equation (4) may be defined as follows:

$$B.C: \begin{cases} C_{11}T_s(a,t)+C_{12}\left.\dfrac{\partial T_s}{\partial r}\right|_{r=a}=g_1 \\ C_{21}T_s(b,t)+C_{22}\left.\dfrac{\partial T_s}{\partial r}\right|_{r=b}=g_2 \end{cases} \tag{6}$$

With Integrating Equation (4):

$$T_s=\frac{C_1}{r}+C_2 \tag{7}$$

The integral constants in Equation (7) are applied as follows:

$$C_1=\frac{C_{21}g_1-C_{11}g_2}{\dfrac{C_{21}}{a^2}(aC_{11}-C_{12})-\dfrac{C_{11}}{b^2}(bC_{21}-C_{22})} \tag{8}$$

$$C_2=\frac{g_1}{C_{11}}-\frac{(C_{21}g_1-C_{11}g_2)\left(\dfrac{1}{a}-\dfrac{C_{12}}{C_{11}a^2}\right)}{\dfrac{C_{21}}{a^2}(aC_{11}-C_{12})-\dfrac{C_{11}}{b^2}(bC_{21}-C_{22})} \tag{9}$$

or:

$$C_2=\frac{g_2}{C_{21}}-\frac{(C_{21}g_1-C_{11}g_2)\left(\dfrac{1}{b}-\dfrac{C_{22}}{C_{21}b^2}\right)}{\dfrac{C_{21}}{a^2}(aC_{11}-C_{12})-\dfrac{C_{11}}{b^2}(bC_{21}-C_{22})} \tag{10}$$

The boundary conditions for Equation (5) may be defined as follows:

$$\begin{cases} B.C: \begin{cases} C_{11}T_h(a,t)+C_{12}\left.\dfrac{\partial T_h}{\partial r}\right|_{r=a}=0 \\ C_{21}T_h(b,t)+C_{22}\left.\dfrac{\partial T_h}{\partial r}\right|_{r=b}=0 \end{cases} \\ I.C: T_h(r,0)=T_i(r)-T_s(r) \end{cases} \tag{11}$$

$T_h(r,t)$ is obtained as follows:

$$T_h(r,t)=\sum_{n=1}^{\infty}C_n f(r,\lambda_n)e^{-\kappa\lambda_n^2 t} \tag{12}$$

where,

$$\begin{aligned} C_n &= \frac{\int_a^b r^2\left(T_i(r)-T_s(r)\right)f(r,\lambda_n)dr}{\|f(r,\lambda_n)\|^2} \\ &= \frac{1}{\|f(r,\lambda_n)\|^2}\left\{\int_a^b r^2 T_i(r)f(r,\lambda_n)dr\right. \\ &-\frac{2\sqrt{b}}{\lambda_n^3}\left[J_{\frac{1}{2}}(\lambda_n b)\left(Ab\lambda_n-B\left(1-\frac{b^2\lambda_n^2}{2}\right)\right)\right. \\ &\left.+J_{\frac{-1}{2}}(\lambda_n b)\left(A\left(1-\frac{b^2\lambda_n^2}{2}\right)+Bb\lambda_n\right)\right] \\ &+\frac{2\sqrt{a}}{\lambda_n^3}\left[J_{\frac{1}{2}}(\lambda_n a)\left(Aa\lambda_n-B\left(1-\frac{a^2\lambda_n^2}{2}\right)\right)\right. \\ &\left.\left.+J_{\frac{-1}{2}}(\lambda_n a)\left(A\left(1-\frac{a^2\lambda_n^2}{2}\right)+Ba\lambda_n\right)\right]\right\} \end{aligned} \tag{13}$$

$f(r,\lambda_n)$ (Eigen-function) is as follows:

$$f(r,\lambda_n)=r^{\frac{-1}{2}}\left(AJ_{\frac{1}{2}}(\lambda_n r)+BJ_{\frac{-1}{2}}(\lambda_n r)\right) \tag{14}$$

Where, $J_{-\frac{1}{2}}$ and $J_{\frac{1}{2}}$ are Bessel functions of the first-kind and of order $\left(-\frac{1}{2}\right),\left(\frac{1}{2}\right)$, respectively.

In addition, λ_n (eigenvalues) are positive roots of the Equation (15).

$$\begin{aligned}&\left[C_{11}J_{\frac{1}{2}}(\lambda_n a)-C_{12}\lambda_n J_{\frac{3}{2}}(\lambda_n a)\right]\\&\times\left[\left(C_{21}-\frac{C_{22}}{b}\right)J_{\frac{-1}{2}}(\lambda_n b)-C_{22}\lambda_n J_{\frac{1}{2}}(\lambda_n b)\right]\\&-\left[C_{21}J_{\frac{1}{2}}(\lambda_n b)-C_{22}\lambda_n J_{\frac{3}{2}}(\lambda_n b)\right]\\&\times\left[\left(C_{11}-\frac{C_{12}}{a}\right)J_{\frac{-1}{2}}(\lambda_n a)-C_{12}\lambda_n J_{\frac{1}{2}}(\lambda_n a)\right]\\&=0\end{aligned}\tag{15}$$

The constant parameters A and B are defined as:

$$\begin{cases}A=\left(C_{11}-\frac{C_{12}}{a}\right)J_{\frac{-1}{2}}(\lambda_n a)\\-C_{12}\lambda_n J_{\frac{1}{2}}(\lambda_n a)\\B=-C_{11}J_{\frac{1}{2}}(\lambda_n a)+C_{12}\lambda_n J_{\frac{3}{2}}(\lambda_n a)\end{cases}\tag{16}$$

or:

$$\begin{cases}A=\left(C_{21}-\frac{C_{22}}{b}\right)J_{\frac{-1}{2}}(\lambda_n b)\\-C_{22}\lambda_n J_{\frac{1}{2}}(\lambda_n b)\\B=-C_{21}J_{\frac{1}{2}}(\lambda_n b)+C_{22}\lambda_n J_{\frac{3}{2}}(\lambda_n b)\end{cases}\tag{17}$$

The norm of Eigen-function $\|f(r,\beta_n)\|^2$ is obtained in the following way:

$$\begin{aligned}&\|f(r,\lambda_n)\|^2=\int_a^b r^2 f^2(r,\lambda_n)\,dr\\&=\frac{b^2}{2}\left[\left(AJ_{\frac{1}{2}}(\lambda_n b)+BJ_{\frac{-1}{2}}(\lambda_n b)\right)^2\right.\\&-A^2\left(J_{\frac{-1}{2}}(\lambda_n b)J_{\frac{3}{2}}(\lambda_n b)\right)\\&-B^2\left(J_{\frac{1}{2}}(\lambda_n b)J_{\frac{-3}{2}}(\lambda_n b)\right)\\&\left.+2AB\left(J_{\frac{1}{2}}(\lambda_n b)J_{\frac{3}{2}}(\lambda_n b)\right)\right]\\&-\frac{a^2}{2}\left[\left(AJ_{\frac{1}{2}}(\lambda_n a)+BJ_{\frac{-1}{2}}(\lambda_n a)\right)^2\right.\\&-A^2\left(J_{\frac{-1}{2}}(\lambda_n a)J_{\frac{3}{2}}(\lambda_n a)\right)\\&-B^2\left(J_{\frac{1}{2}}(\lambda_n a)J_{\frac{-3}{2}}(\lambda_n a)\right)\\&\left.+2AB\left(J_{\frac{1}{2}}(\lambda_n a)J_{\frac{3}{2}}(\lambda_n a)\right)\right]\end{aligned}\tag{18}$$

Finally, the temperature distribution is obtained as follows:

$$T(r,t)=T_s(r)+\sum_{n=1}^{\infty}C_n f(r,\lambda_n)e^{-\kappa\lambda^2 t}\tag{19}$$

3. Transient Thermoelastic Formulation

In the spherical symmetry condition, the strain-displacement equations are:

$$\begin{cases}\varepsilon_{\phi\phi}=\varepsilon_{\theta\theta}=\frac{u_r}{r}\\\varepsilon_{rr}=\frac{\partial u_r}{\partial r}\end{cases}\tag{20}$$

and the stress-strain equations are:

$$\begin{aligned}\sigma_{rr}&=\frac{E}{(1+\nu)(1-2\nu)}\left((1-\nu)\frac{\partial u_r}{\partial r}+2\nu\frac{u_r}{r}\right.\\&\left.-(1+\nu)\alpha T\right)\end{aligned}\tag{21}$$

$$\begin{aligned}\sigma_{\phi\phi}&=\sigma_{\theta\theta}=\frac{E}{(1+\nu)(1-2\nu)}\left(\frac{u_r}{r}+\nu\frac{\partial u_r}{\partial r}\right.\\&\left.-(1+\nu)\alpha T\right)\\T&=T(r,t)-T_0\end{aligned}\tag{22}$$

Where, E, α, ν are young modulus, coefficient of linear thermal expansion, and Poisson's ratio, respectively. In addition, σ_{rr} and $\sigma_{\phi\phi}$ are radial and circumferential stresses components, and T_0 is reference temperature which in this study is assumed having zero value.

The equilibrium equation is as follows:

$$\frac{\partial\sigma_{rr}}{\partial r}+2\frac{\sigma_{rr}-\sigma_{\phi\phi}}{r}=0\tag{23}$$

Using Equations (20),(21) and (23):

$$\frac{\partial}{\partial r}\left(\frac{1}{r^2}\frac{\partial(u_r r^2)}{\partial r}\right)=\frac{1+\nu}{1-\nu}\alpha\frac{\partial T}{\partial r}\tag{24}$$

With integrating Equation (24):

$$\begin{aligned}u_r(r,t)&=Ar+\frac{B}{r^2}+\\&\frac{1+\nu}{1-\nu}\frac{\alpha}{r^2}\int_a^r r^2 T(r,t)\,dr\end{aligned}\tag{25}$$

σ_{rr} and $\sigma_{\phi\phi}$ are obtained with substituting Equation (25) into Equation (20),(21):

$$\begin{aligned}\sigma_{rr}&=C_1^*-\frac{2C_2^*}{r^3}\\&-\frac{2\alpha E}{1-\nu}\frac{1}{r^3}\int_a^r r^2 T(r,t)\,dr\end{aligned}\tag{26}$$

$$\sigma_{\phi\phi} = \sigma_{\theta\theta} = C_1^* + \frac{C_2^*}{r^3} + \frac{\alpha E}{1-\nu}\left(\frac{1}{r^3}\int_a^r r^2 T(r,t)\,dr - T(r,t)\right) \quad (27)$$

Where,

$$\begin{cases} C_1^* = \dfrac{AE}{1-2\nu} \\ C_2^* = \dfrac{BE}{1+\nu} \end{cases} \quad (28)$$

In this paper, the hollow sphere is subjected to pressures P_a and P_b at the inner and external surfaces, respectively:

$$\begin{cases} \sigma_{rr}(r=a) = -P_a \\ \sigma_{rr}(r=b) = -P_b \end{cases} \quad (29)$$

With substituting boundary conditions (Equation (29)) into Equation (26), C_1^* and C_2^* are obtained as follows:

$$C_1^* = \frac{1}{b^3-a^3}\left(P_a a^3 - P_b b^3 + \frac{2\alpha E}{1-\nu}\int_a^b r^2 T(r,t)\,dr\right) \quad (30)$$

$$C_2^* = \frac{a^3 b^3}{2\left(b^3-a^3\right)}\left(P_a - P_b + \frac{2\alpha E}{1-\nu}\frac{1}{b^3}\int_a^b r^2 T(r,t)\,dr\right) \quad (31)$$

Where,

$$\int_a^r r^2 T(r,t)\,dr = \frac{C_1}{2}r^2 + \frac{C_2}{3}r^3 + \sum_{n=1}^{\infty} C_n e^{-\kappa\lambda_n^2 t}\left(\frac{\sqrt{r}}{\lambda_n^2}\left[A\left(J_{\frac{1}{2}}(r\lambda_n) - r\lambda_n J_{\frac{-1}{2}}(r\lambda_n)\right) + B\left(J_{\frac{-1}{2}}(r\lambda_n) + r\lambda_n J_{\frac{1}{2}}(r\lambda_n)\right)\right] - \frac{\sqrt{a}}{\lambda_n^2}\left[A\left(J_{\frac{1}{2}}(a\lambda_n) - a\lambda_n J_{\frac{-1}{2}}(a\lambda_n)\right) + B\left(J_{\frac{-1}{2}}(a\lambda_n) + a\lambda_n J_{\frac{1}{2}}(a\lambda_n)\right)\right]\right) \quad (32)$$

4. Results and Discussion

Consider a sphere with properties as follows

$a = 0.4$ m, $b = 0.6$ m, $E = 200$ GPa, $\nu = 0.3$
$P_a = 70$ MPa, $P_b = 70$ MPa, $\rho = 7854$ Kg/m^3
$\alpha = 1.17\left(10^{-5}\right)$ 1/°C, $k = 60.5$ W/m.K
and $C_p = 434$ J/Kg.K

Assume that the internal and external surfaces of the shell are under heat flux and convection, respectively. In addition the initial condition is also as a linear function in terms of the radius. Therefore:

$$\begin{cases} B.C \quad : \begin{cases} -k\left.\dfrac{\partial T}{\partial r}\right|_{r=a} = q \\ -k\left.\dfrac{\partial T}{\partial r}\right|_{r=b} = h\left(T(b,t) - T_\infty\right) \end{cases} \\ I.C \quad : \quad T(r,0) = T_i(r) \end{cases} \quad (33)$$

Using Equation (6)-(9) and Equation (33) the temperature distribution is obtained as follows:

$$T_s(r) = T_\infty + \frac{qa^2}{k}\left(\frac{1}{r} - \frac{1}{b} + \frac{k}{b^2 h}\right)$$

and:

$$\begin{cases} A = \dfrac{k}{a} J_{\frac{-1}{2}}(\lambda_n a) + k\lambda_n J_{\frac{1}{2}}(\lambda_n a) \\ B = -k\lambda_n J_{\frac{3}{2}}(\lambda_n a) \end{cases}$$

Here λ_n are positive roots of the following equation:

$$\left[hJ_{\frac{1}{2}}(\lambda_n b) - k\lambda_n J_{\frac{3}{2}}(\lambda_n b)\right] \times \left[\frac{k}{a}J_{\frac{-1}{2}}(\lambda_n a) + k\lambda_n J_{\frac{1}{2}}(\lambda_n a)\right] - \left[\left(h - \frac{k}{b}\right)J_{\frac{-1}{2}}(\lambda_n b) - k\lambda_n J_{\frac{1}{2}}(\lambda_n b)\right] \times k\lambda_n J_{\frac{3}{2}}(\lambda_n a) = 0$$

The numerical parameters are presented as follows:

$$q = 500\frac{W}{m^2} \quad , \quad T_i(r) = \frac{1}{r}$$
$$T_\infty = 15°C \quad , \quad h = 25\frac{W}{m^2.K}$$

Figure 1 shows temperature distribution for the course of 3600 seconds. The distribution of temperature at t = 3600sec is shown in Figure 2. The temperature distribution for different radii versus time is indicated in Figure 3. The temperature decreases whereas radius increases. The temperature distribution for different times versus radius is indicated in Figure 4. This Figure show that temperature increases as time increases.

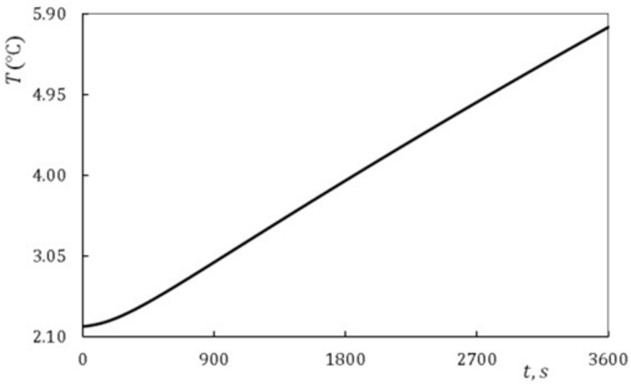

Figure 1. Distribution of temperature versus time for r = 0.45 m.

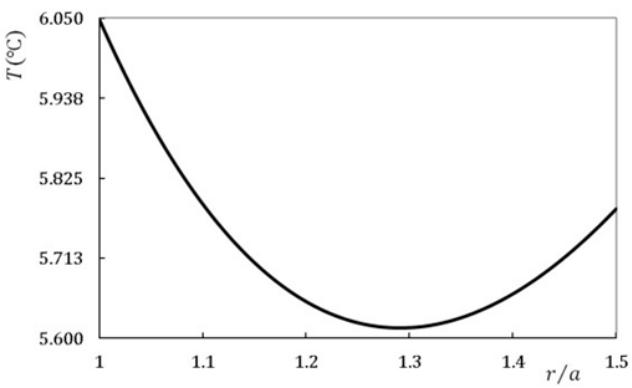

Figure 2. Distribution of temperature versus radius at t = 3600sec.

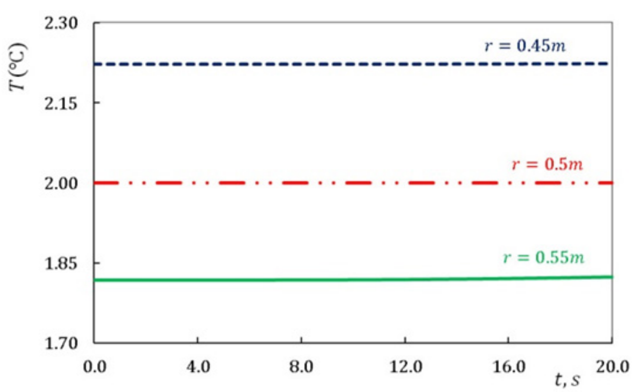

Figure 3. Distribution of temperature for various radii versus time.

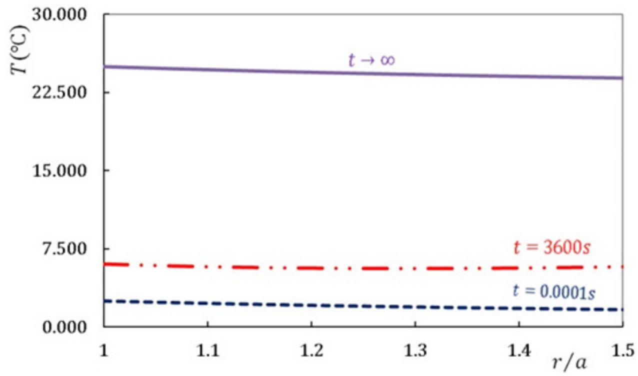

Figure 4. Distribution of temperature for various times versus radius.

Figures 5 to 7 provide an illustration of the distributions of radial displacement, radial and circumferential stresses vs. radial direction. Moreover, Figure 8 to 10 shows the distributions of radial displacement, radial and circumferential stresses vs. time. As could be seen in Figure 8, the radial displacement increases when time increases. Figure 9 shows that at first, radial stresses decreases and then it increases as time increases whereas in Figure 10 for circumferential stress this situation is reversed.

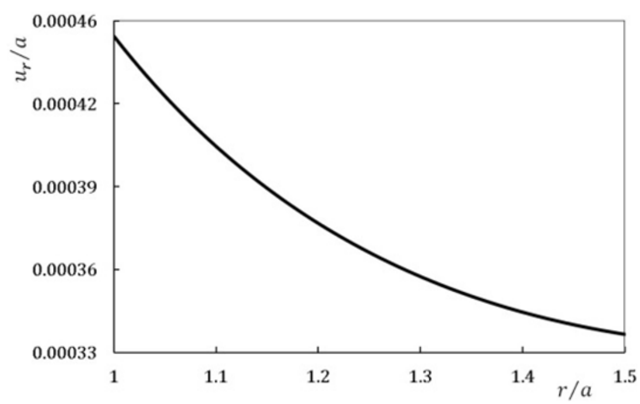

Figure 5. Distribution of radial displacement versus radius at t = 3600 sec.

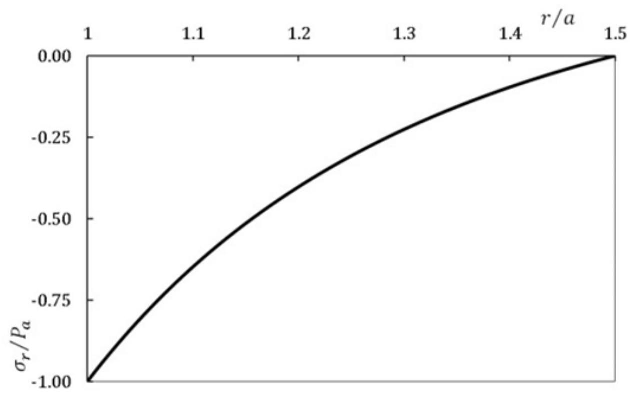

Figure 6. Distribution of radial stress versus radius at t = 3600 sec.

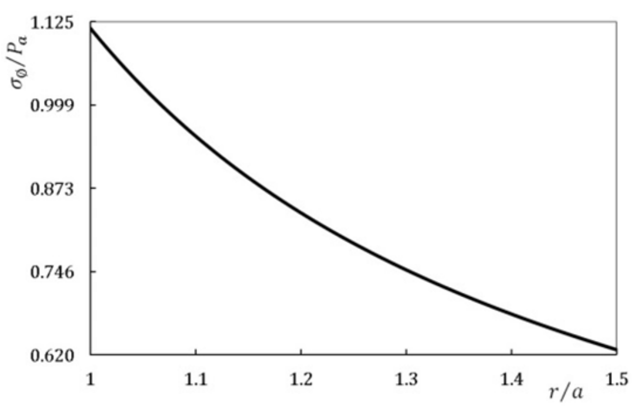

Figure 7. Circumferential distribution of stress versus radius at t = 3600 sec.

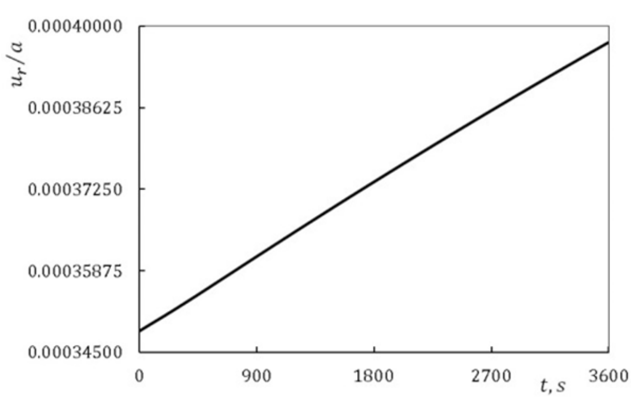

Figure 8. Distribution of radial displacement versus time in r = 0.45 m.

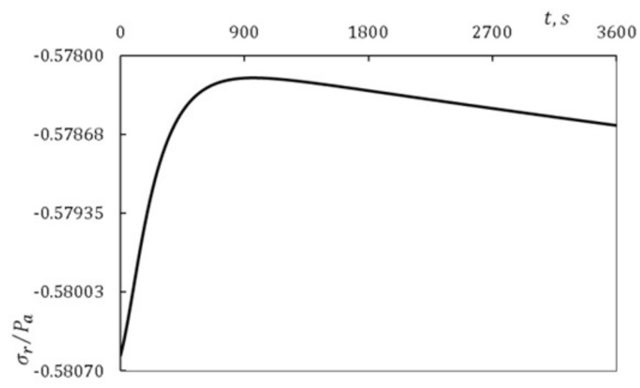

Figure 9. Distribution of radial stress versus time in r = 0.45 m.

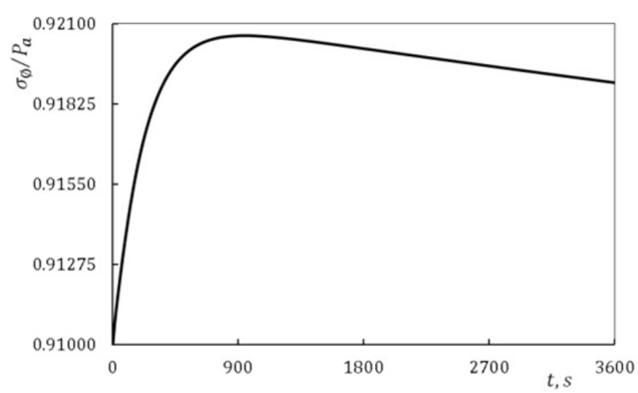

Figure 10. Distribution of circumferential stress versus time in r = 0.45 m.

The comparison distribution of radial displacement and stress for various time and radii are shown in Figures 11 to 14. In these Figures, radial displacement, radial and circumferential stresses decrease in as radius increases whereas this situation for different times is reversed.

Figures 15 and 16 show that values change of radial and circumferential stresses are very small while the time increases.

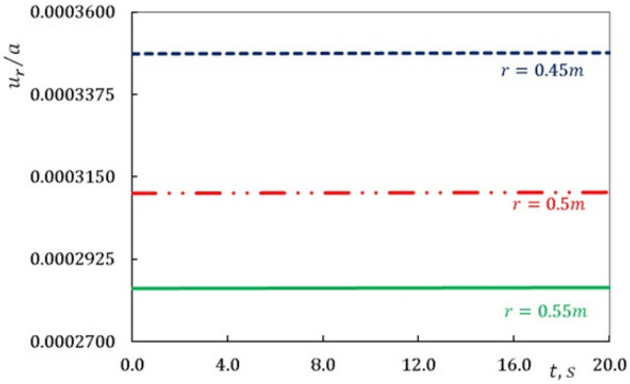

Figure 11. The compare of distribution of radial displacement for various radii versus time.

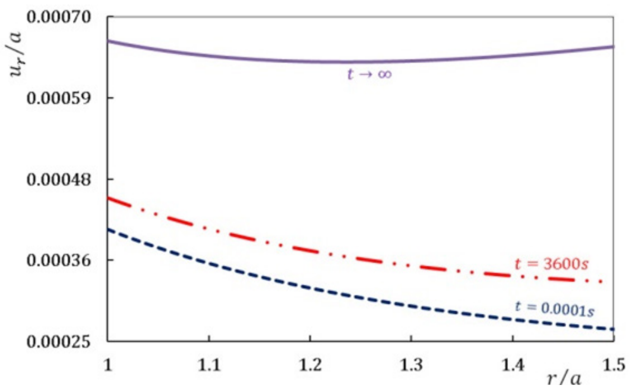

Figure 12. The compare of distribution of radial displacement for various times versus radius.

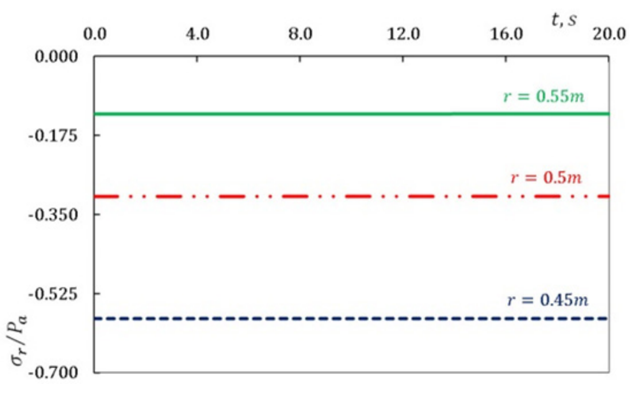

Figure 13. The compare of distribution of radial stress for various radii versus time.

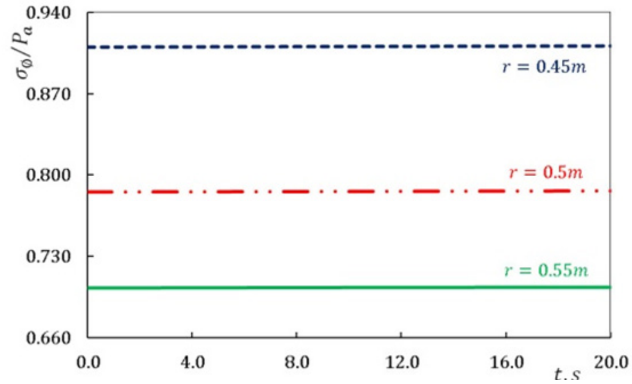

Figure 14. The compare of distribution of circumferential stress for various radii versus time.

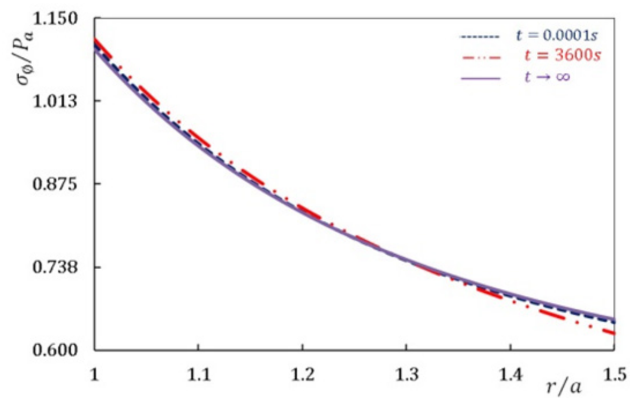

Figure 15. The compare of distribution of circumferential stress for various times versus radius.

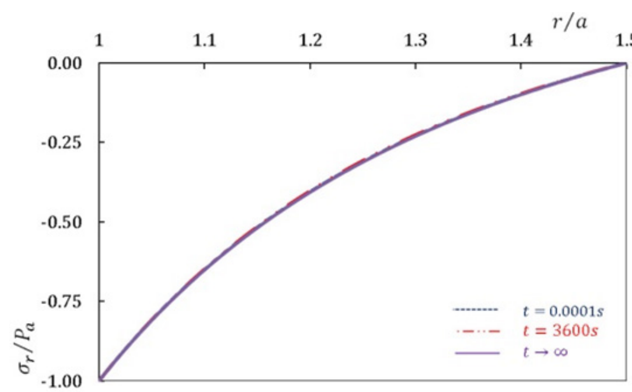

Figure 16. The compare of distribution of circumferential stress for various times versus radius.

5. Conclusions

In this paper, using the infinitesimal theory of elasticity, thermo-elastic analysis in the transient condition of a thick pressurized sphere under general boundary conditions is presented. The material properties are isotropic and homogeneous. The temperature distribution is versus time and radius. The numerical results show that time and temperature has a significant effect on displacement and stresses.

6. References

1. Cheung JB, Chen TS, Thirumalai K. Transient thermal stresses in a sphere by local heating. Journal of Applied Mechanics. 1974; 41(4):930–4.
2. Tanigawa Y, Takeuti Y, Ueshima K. Transient thermal stresses of solid and hollow spheres with spherically isotropic thermoelastic properties. Archive of Applied Mechanics. 1984; 54(4):259–67.
3. Toshiaki H. Thermal shock in hollow sphere caused by rapid uniform heating. Journal of Applied Mechanics. 1991; 58(1):64–9.
4. Abd-Aalla AM, Abd-Alla AN, Zeidan NA. Transient thermal stresses in a spherically orthotropic elastic medium with spherical cavity. Applied Mathematics and Computation. 1999; 105(2-3):231–52.
5. Jordan PM, Puri P. Thermal stresses in a spherical shell under three thermoelastic models. Journal of Thermal Stresses. 2001; 24(1):47–70.
6. Bagri A, Eslami MR. Analysis of thermoelastic waves in functionally graded hollow spheres based on the green-lindsay theory. Journal of Thermal Stresses. 2007; 30(12):1175–93.
7. Tutuncu N, Temel B. A novel approach to stress analysis of pressurized FGM cylinders, disks and spheres. Composite Structures. 2009; 91(3):385–90.
8. Ootao Y. Transient thermoelastic analysis for a multilayered hollow sphere with piecewise power law nonhomogeneity. Composite Structures. 2011; 93(7):1717–25.
9. Nejad MZ, Afshin A. Thermoelastic transient response of rotating thick cylindrical shells under general boundary conditions. International Research Journal of Applied and Basic Sciences. 2013; 4(9):2796–809.
10. Nejad MZ, Afshin A. Transient thermoelastic analysis of pressurized rotating disks subjected to arbitrary boundary and initial conditions. Chinese Journal of Engineering. 2014. DOI: 10.1155/2014/894902.